

# Synthesis of nano-sized gadolinia doped ceria powder by aerosol flame deposition

Jong Mo Im, Hyun Jin You, Yong Sub Yoon, Dong Wook Shin\*

*Division of Materials Science & Engineering, Hanyang University, 17 Haengdang-dong, Seongdong-gu, Seoul 133-791, Republic of Korea*

Available online 23 March 2007

## Abstract

In this work, aerosol flame deposition method was applied to deposit spherical and dense gadolinia-doped ceria (GDC) particles in the sub-micron range for the electrolyte application in solid oxide fuel cell. The particle size distribution was dependent on processing parameters such as the concentration of the precursor solution, the hydrogen gas flow rate, the oxygen gas flow rate, and flame conditions. GDC electrolyte thin layer was also fabricated from the liquid source materials by AFD method. Microstructure of synthesized powder was characterized using XRD and SEM. © 2007 Elsevier Ltd. All rights reserved.

*Keywords:* Aerosol flame deposition; Nanocomposites; CeO<sub>2</sub>; Fuel cells

## 1. Introduction

High operation temperature at around 800–1000 °C is the main disadvantage of a solid oxide fuel cell (SOFC) that gives rise to its safety and maintenance issues. Different approaches to this problem solution have been attempted<sup>1</sup> and the operation temperature tends to reduce recently. Among various methods to reduce operation temperature, the application of thin film electrolyte is leading to the enhanced effectiveness if an alternative material of higher ionic conductivity at lower temperatures is employed.<sup>2,3</sup> For the purpose of decreasing the electrolyte thickness to reduce operating temperature, Gauckler reported a new approach in fabricating thin film of oxides.<sup>4</sup> The thin film fabrication methods can be classified into chemical methods, physical methods and ceramic powder process.<sup>4</sup> The chemical method comprises the sol–gel process and the physical method includes the sputtering. Ceramic powder process is traditional solid-state reaction method, in which the powder mixed with a binder is sintered at high temperature. Unlike these film preparation techniques, the AFD (aerosol flame deposition) process is unique since it offers a route to prepare nano-porous film composed of nano-sized particles. Compared with other thin-film deposition techniques such as chemical vapor deposition (CVD),<sup>5,6</sup> sol–gel process<sup>7</sup> and other spray pyrolysis techniques,<sup>8,9</sup> the

advantages of this technique are a wide choice of nonvolatile precursors including liquid precursors, high degree of crystallinity of as-prepared metal oxide nanoparticles<sup>10,11</sup> due to its high reaction temperatures (1727–2727 °C), and the capability to produce virtually all kinds of oxide nano-powders which have been synthesized by solid state reactions. This method also enables the thin film deposition in ambient atmosphere even if an additional heat treatment is required to produce dense film.

In this work, the aerosol flame deposition method was applied for the first time to deposit ceria powder in order to prepare thin film type electrolyte for SOFC. Detailed investigation of the effects of deposition parameters on the microstructure and the particle size distribution of gadolinia-doped ceria (GDC) particles synthesized will be also reported.

## 2. Experimental procedures

Schematically shown in Fig. 1 is the AFD (aerosol flame deposition) system employed in this work. In the AFD process, a liquid precursor solution was prepared by dissolving the desired precursors into a solvent and then atomized into micro-sized droplets by ultrasonic nebulizer with a 1.7 MHz resonator. The atomized droplets were carried by Ar carrier gas into a flame hydrolysis reaction zone in an oxy-hydrogen torch. The essential part of the system is the oxy-hydrogen torch, which is made from four concentric tubes creating three concentric gaps, and one shield tube keeping flame stable. Precursor solution flows through the centermost tube of the torch while hydrogen,

\* Corresponding author. Tel.: +82 2 2220 0503; fax: +82 2 2299 3851.  
E-mail address: [dwshin@hanyang.ac.kr](mailto:dwshin@hanyang.ac.kr) (D.W. Shin).

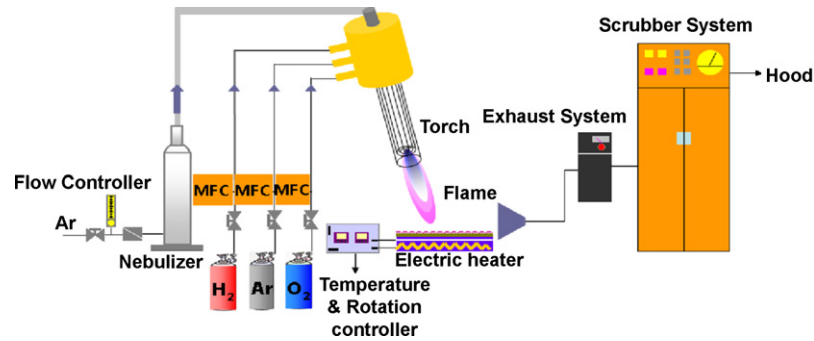


Fig. 1. A schematic diagram of experimental apparatus for the synthesis of GDC by aerosol flame deposition.

argon and oxygen flow through three gaps having different width to ensure laminar flow of gases. For preparing precursor solution, Cerium nitrate hexahydrate,  $\text{Ce}(\text{NO}_3)_3 \cdot 6\text{H}_2\text{O}$  [Aldrich, >99.9%] and gadolinium nitrate hexahydrate,  $\text{Gd}(\text{NO}_3)_3 \cdot 6\text{H}_2\text{O}$  [Aldrich, >99.9%] were used as precursors and then ultrasonically agitated in methanol [CARLO ERBA, >95.0%] at room temperature to obtain a 0.05 M  $\text{Gd}_{0.1}\text{Ce}_{0.9}\text{O}_{2-x}$  solution. The microscopic features of the GDC particles synthesized as a function of the hydrogen flow rate (1.0–5.0 l/min), the oxygen flow rate (4.5–12.0 l/min) and solution mole concentration (0.01–1.0 M) were characterized in plan-view and in cross-section using a scanning electron microscope (JEOL, JSM-6330F). For investigating the phase and crystallinity of the synthesized powders, X-ray diffraction was measured by Rigaku M2500 diffractometer with a scanning step of  $0.014^\circ$ , a scanning time of 0.05 s per step and an angle range from  $20$ – $90^\circ$ .

### 3. Results and discussion

The spherical  $\text{Gd}_{0.1}\text{Ce}_{0.9}\text{O}_{2-x}$  particles with smooth surface were deposited and the as-prepared powder was composed of particles with two different size distributions. Smaller particles

were a few tens of nanometers in diameter and larger particles were approximately a few hundreds of nanometer in diameter, as shown in Fig. 2(b). The particles diameter distribution of  $\text{Gd}_{0.1}\text{Ce}_{0.9}\text{O}_{2-x}$  powder revealed a bimodal size distribution, consisting of both nano-particles and sub-micron particles. The origin of this bimodal distribution is thought to be two different mechanisms of particle formation. Large particle is formed by the rapid evaporation of liquid solvent in high temperature flame and pyrolysis mechanism of dissolved precursors. This mechanism is similar to that of conventional spray pyrolysis. The particle size is strongly dependent on the aerosol droplet size and the precursor concentration.<sup>12</sup> Small particle might be formed by the plasma reaction. In an oxy-hydrogen flame, some of ions in the precursor solution do not have enough time to go through the pyrolysis process. Instead, they could remain as ions after the complete evaporation of solvent, and consequently form gaseous thermal plasma. The plasma gases will be supersaturated at the region of lower temperature, and experience the gaseous nuclear and growth process. The nucleation rate will be dependent on the supersaturation of plasma gas phases and this supersaturation increases at the end of flame due to reduced temperature. The Brownian coagulation would happen during

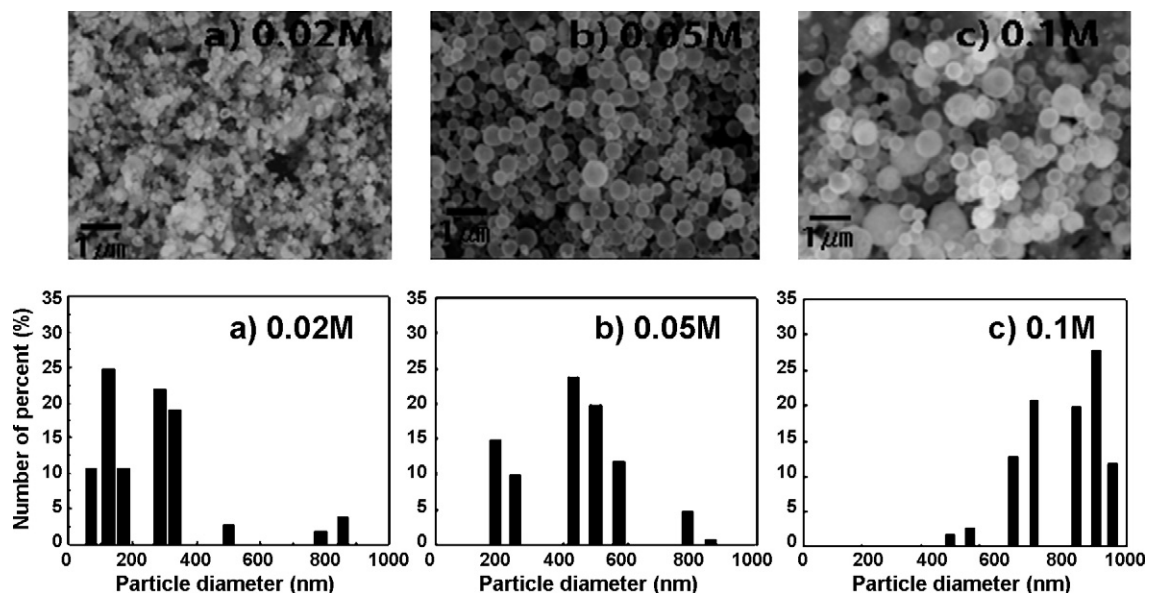


Fig. 2. SEM images and particle size distribution of GDC as-deposits synthesized by AFD at various precursor solution mole concentration with fixed hydrogen gas flow rate of 4.5 l/min and oxygen gas flow rate of 7.5 l/min. The images were taken from the as-deposited state.

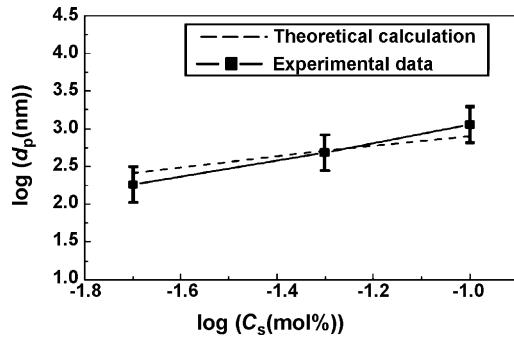


Fig. 3. The variation of mean particle size as a function of precursor solution concentration. The dotted line is the theoretical calculation by Lang's model. Theoretically calculated result was adjusted by a constant to match the experimental data.

the random flow of solid particles within the flame and cause the agglomeration of small particles. It was observed that the small particle tends to agglomerate in higher degree compared to large particles.

Since two kinds of particles are formed by different mechanisms, the effects of process parameters differ in each kind of particles. The particle size distribution and the surface images of the synthesized  $\text{Gd}_{0.1}\text{Ce}_{0.9}\text{O}_{2-x}$  particles were studied in the solution concentration range of 0.01–0.1 M and summarized in Fig. 2. From the SEM micrographs, one can see that the average size of large particles increased and the small particles gradually disappeared with increasing concentration of precursor solution. The average particle size of large one increased approximately from 6 to 95%. The proportion of the small one decreased approximately from 90 to almost 0%. The size of particle formed by the pyrolysis mechanism is largely depending on the aerosol droplet size and the concentration of source liquid as predicted by Lang.<sup>13</sup> Once the droplet size of aerosol,  $D_{\text{droplet}}$ , generated by ultrasonic nebulizer is determined, the size of particle,  $d_p$ , transformed from this aerosol droplet is expressed by

the Lang's theory,

$$d_p = \left[ \frac{MC_s}{1000\rho_s} \right]^{1/3} D_{\text{droplet}} \quad (1)$$

where  $M$  and  $\rho_s$  are the molecular weight and theoretical density of the particle material, and  $C_s$  is the concentration of source materials in the precursor solution. This equation assumes that there is no complex aerosol dynamics such as the breaking up of large droplets and Brownian coagulations of particles. In Fig. 3, the concentration dependence of particle size is compared to Eq. (1) and one can see that theory predicts successfully the variation of mean particle size as a function of  $C_s$ . Nevertheless, the concentration dependency (the slope of linear fitted line) was slightly lower than 1/3 and this suggests that there are other parameters determining the particle size in the real experiments such as the change of the viscosity of precursor solution, breaking up of droplet, the coagulation of particles within the flame. However, it is clear that the particle size can be controlled by simply changing the concentration of precursor solution. The fitted result in Fig. 3 also suggests that the aerosol breaking and the particle coagulation do not strongly affect the final size of particle formed by the pyrolysis mechanism.

The effects of hydrogen gas flow rate on the microstructure and size distribution of the GDC particles synthesized were investigated in the hydrogen gas flow rate range of 1.5–4.5 l/min and the results were shown in Fig. 4. The increment of hydrogen gas flow rate increases the temperature and length of flame, which results in the increase of temperature of the deposition spot. Therefore, the small particle produced by the nucleation and growth mechanism has less chance to nucleate due to lower supersaturation at the deposition position. This tendency is clearly shown in Fig. 4, where the number of small particles decreases dramatically with the increasing hydrogen flow rate. In other hands, the size of large particles gradually increased

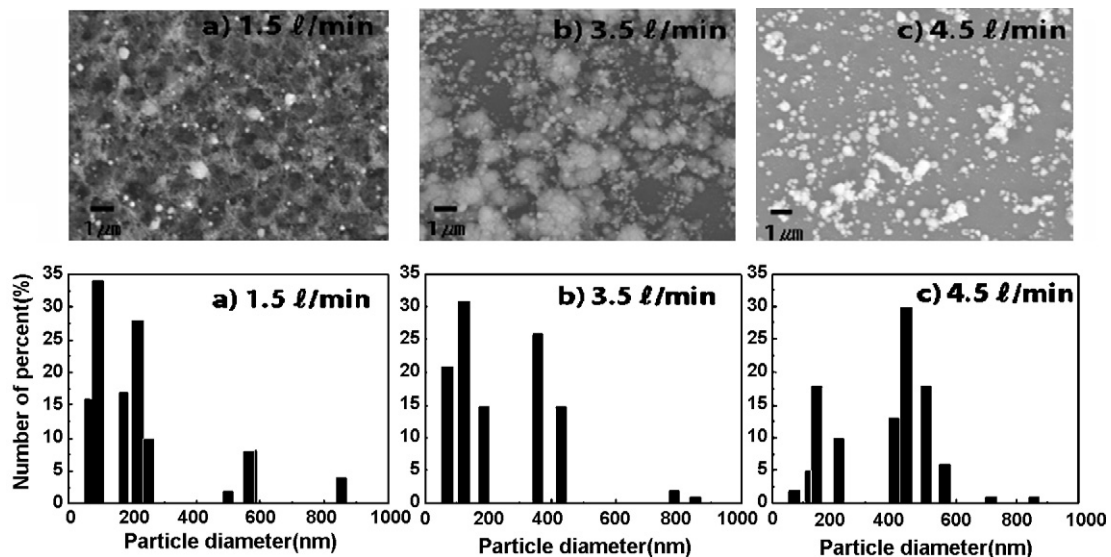


Fig. 4. SEM images and particle size distribution of GDC powder synthesized by AFD at various hydrogen dispersion gas flow rate with fixed solution concentration of 0.05 M and oxygen gas flow rate of 7.5 l/min. The specimen was prepared by dispersing powders in the methanol and sprayed onto Si wafer.

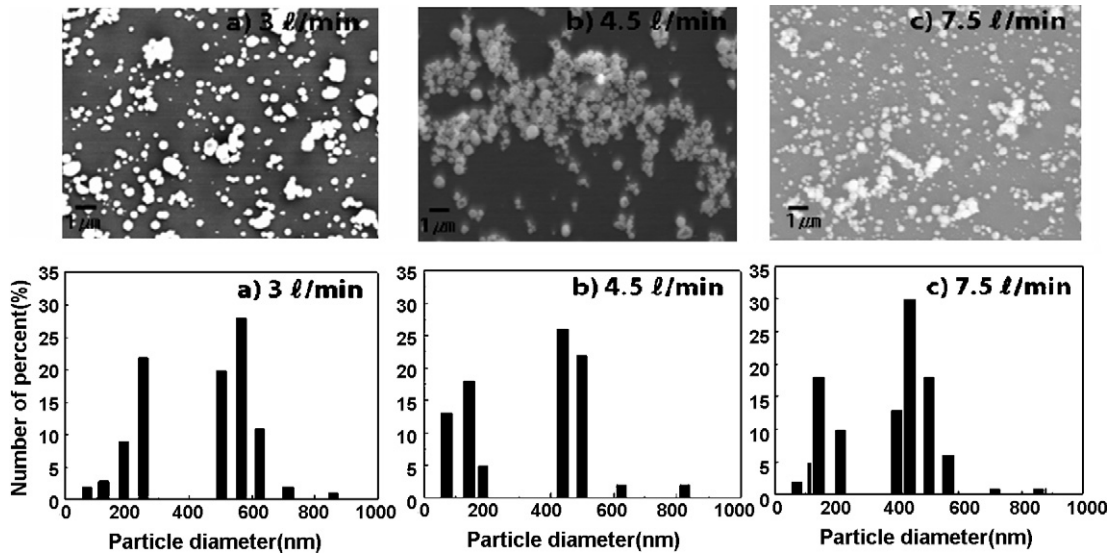


Fig. 5. SEM images and particle size distribution of GDC powder synthesized by AFD at various oxygen dispersion gas flow rate with solution concentration of 0.05 M and hydrogen gas flow rate of 4.5 l/min. The specimen was prepared by dispersing powders in the methanol and sprayed onto Si wafer. Though (c) is identical to Fig. 4(c), it is used again for the comparison purpose.

with the increasing flow of hydrogen gas. This is believed due to the increased residence time of particle in the prolonged flame and hence, the increased chance of particle growth by the heterogeneous nucleation at the surface of particle.

The effect of the oxygen gas flow rate on the microstructure and size distribution of the synthesized GDC particles is less obvious compared to that of the hydrogen gas flow rate. As shown in Fig. 5, the size of large particles tends to decrease slightly. This tendency is attributed to the slight decrease of flame temperature caused by the excessive flow of oxygen over the optimum ratio to the hydrogen gas. This is consistent with the effect of oxygen gas flow rate in synthesis of silica in turbulent diffusion flame reactor.<sup>14,15</sup> The hydrogen gas flow rate and oxygen flow gas rate may balance and compensate for each other for attainment for a specific particle size and to make flame stable.

Based on the experimental results under various conditions, the optimum condition for the deposition was determined to precursor solution concentration of 0.05 M, hydrogen flow rate of 4.5 l/min and oxygen flow rate of 7.5 l/min. These conditions were confirmed to synthesize dense particles in stable flame and produce substantial deposition rate. However, the optimum condition for the synthesis is greatly affected by the

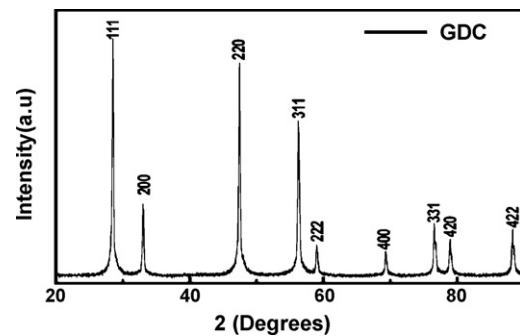


Fig. 6. XRD pattern of GDC powder synthesized at H<sub>2</sub> flow rate 4.5 l/min, O<sub>2</sub> flow rate 7.5 l/min, Ar flow rate 1 l/min, turn table temperature at 160 °C, precursor concentration 0.05 mol% on Si wafer substrate.

system geometry such as torch and aerosol generation system (nebulizer).

Mahata and Das<sup>16</sup> reported that the lattice parameter has been found to increase with Gd<sub>2</sub>O<sub>3</sub> content following Vegard's law. The relationship can be expressed as,

$$a(\text{\AA}) = 5.40606 + 0.00206X \quad (2)$$

where  $X$  (10 mol%) is the mol% of Gd<sub>2</sub>O<sub>3</sub>.

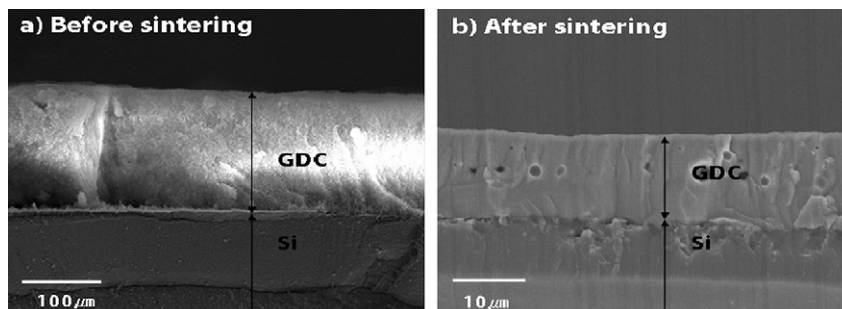


Fig. 7. Cross-sectional SEM images of GDC powder synthesized by AFD before and after heated at 1400 °C for 10 h.

Since the lattice parameter calculated from XRD patterns shown in Fig. 6 is almost same to that of lattice parameters calculated from Mahata's formula (Eq. (2)), it can be assumed that a fully crystallized cubic phase gadolinium doped ceria was successfully synthesized directly from the liquid precursor solution.

Cross-sectional SEM images of the GDC soot deposited on a Si wafer are shown in Fig. 7. The thickness of soot layer was more than 100  $\mu\text{m}$  and the deposition rate was approximately 0.8  $\mu\text{m}/\text{min}$ . After this soot layer was sintered at 1400  $^{\circ}\text{C}$  for 10 h as shown in Fig. 7(b), the soot layer converted into dense film and the thickness of the layer decreased to 10  $\mu\text{m}$ . The volume shrinkage ratio was approximately 10.

#### 4. Conclusions

The aerosol flame deposition technique was applied to synthesize the GDC nano-sized powder and it was demonstrated that this technique is extremely useful for the production of micron and sub-micron GDC powders and film. The synthesized GDC particles were spherical, solid (dense), and free of agglomeration. The synthesized particles exhibited bimodal size distribution reflecting that two distinct mechanisms are working and the effects of process parameters on these two types of particles were dissimilar. Therefore, the process control should be different to achieve the desired microstructure. Aerosol flame deposition technique is believed to be a promising method for the synthesis of nano-sized GDC powders for SOFC electrolyte. However, the porosity of soot film should be low enough and smaller particle size is required in order to improve the quality of sintered dense film.

#### Acknowledgements

This work was supported by the Seoul Research and Business Development Program (Grant No.10583).

#### References

1. Boivin, J. C. and Mairesse, G., Recent material development in fast oxide ion conductors. *J. Chem. Mater.*, 1998, **10**, 2870–2888.
2. Peng, R. and Xia, C., Intermediate-temperature SOFCs with thin  $\text{Ce}_{0.8}\text{Y}_{0.2}\text{O}_{1.9}$  films prepared by screen-printing. *Solid State Ionics*, 2002, **152/153**, 561–565.
3. Madler, L. and Stark, W. J., Flame-made ceria nanoparticles. *J. Mater. Res.*, 2002, **17**, 1356–1362.
4. Will, J. and Gauckler, L. J., Fabrication of thin electrolytes for second-generation solid oxide fuel cells. *Solid State Ionics*, 2000, **131**, 79–96.
5. Takahashi, Y. and Kawae, T., Chemical vapour deposition of undoped and spinel-doped cubic zirconia film using organometallic process. *J. Cryst. Growth*, 1986, **74**, 409.
6. Chen, H. and Xu, R., Large scale fluorine doped textured transparent conducting  $\text{SnO}_2$  films deposited by atmospheric pressure chemical vapour deposition. *Thin Solid Films*, 1997, **298**, 151–155.
7. Mehta, K. and Xu, R., Two-layer fuel cell electrolyte structure by sol-gel processing. *J. Sol-Gel. Soc. Tech.*, 1998, **11**, 203–207.
8. Wang, S. and Wang, W., Preparation and characterization of cerium(IV) oxide thin film by spray pyrolysis method. *Solid State Ionics*, 2000, **133**, 211–215.
9. Setoguchi, T. and Sawano, M., Application of the stabilized zirconia thin film prepared by spray pyrolysis method to SOFC. *Solid State Ionics*, 1990, **40/41**, 502–505.
10. Pratsinis, S. E. and Vemury, S., Particle formation in gases: a review. *Powder Technol.*, 1996, **88**, 267–273.
11. Takao, T. and Akane, K., Effect of solvent on powder characteristics of zinc oxide and magnesia prepared by flame spray pyrolysis. *J. Ceram. Soc. Jpn.*, 2005, **113**, 255–258.
12. Charojrochkul, S. and Choy, K. L., Flame assisted deposition of cathode for solid oxide fuel cells. 1. Microstructure control from processing parameters. *J. Eur. Ceram. Soc.*, 2004, **24**, 2515–2526.
13. Yuan, F. L. and Chen, C. H., Preparation of zirconia and yttria-stabilized zirconia (YSZ) fine powders by flame-assisted ultrasonic spray pyrolysis (FAUSP). *Solid State Ionics*, 1998, **109**, 119–123.
14. Stark, W. J. and Baiker, A., Flame made titania/silica epoxidation catalysts. *J. Catal.*, 2001, **203**, 516–524.
15. Briesen, H. and Fuhrmann, A., The effect of precursor in flame synthesis of  $\text{SiO}_2$ . *Chem. Eng. Sci.*, 1998, **53**, 4105–4112.
16. Mahata, T. and Das, G., Combustion synthesis of gadolinia doped ceria powder. *J. Alloys Comp.*, 2005, **391**, 129–135.